Designing Log- aesthetic Splines with G^2 Continuity

Kenjiro T. Miura[1], Dai Shibuya[2], R.U. Gobithaasan[3] and Shin Usuki[4]

[1]Shizuoka University, ktmiura@ipc.shizuoka.ac.jp
[2]Shizuoka University, f0230033@ipc.shizuoka.ac.jp
[3]University of Malaysia, Terengganu, gr@umt.edu.my
[4]Shizuoka University, dsusuki@ipc.shizuoka.ac.jp

ABSTRACT

This paper elucidates the possibilities to interactively generate and deform Log-aesthetic (LA) curves regardless of their integral form. The methods proposed are twofold; in the first section, we propose new method to generate an S-shaped LA spline. In the next section, we propose a novel method to solve the G^2 Hermite interpolation problem with LA curves which is in the form of LA triplets. These methods have been implemented as a plug-in module for a commercial CAD system and are successfully used for practical design. This paper proofs that LA curve has matured and ready for industrial design.

1   INTRODUCTION

Recent advancement on Log Aesthetic (LA) curve has been promising and it is now maturing for industrial and graphical design practices. Designers may specify two shape parameters which can be used to generate visually pleasing curves using LA curves. The shape parameters are denoted as α and Λ. The α shape parameter is used to dictate the types of curves the designer wants, e.g., when $\alpha = -1$, the LA curve becomes clothoid and when $\alpha = 2$ the LA curve becomes circle involute. The Λ shape parameter can be used to control certain shape constraints to be satisfied during design processes, e.g. controlling the curvature radius at endpoints.

An independent research indicated that LA curve is the most promising curve for aesthetic design [8]. Recent researches on the LA curve include reformulation of LA curve using variational principles to obtain minimized functionals for free-form surfaces design [14]. In 2009, Gobithaasan and Miura [2] formulated the generalized log-aesthetic curve (GLAC) in a standard form by representing the gradient of the Logarithmic Curvature Graph (LCG) as a function of its arc length. They also reported that the LCG gradient of Generalized Cornu spiral [5] can be written as a linear function [3]. In 2012, Ziatdnov et al. [18] showed that some LA curves can be expressed by incomplete Gamma functions analytically which shortens the computation time up to 10 times. Recently Meek et al. [10] proved that an unique solution exists for G^1 interpolation by using an LA curve segment when $\alpha < 0$.

This paper proposes a novel method to solve G^2 Hermite interpolation problem using LA curves. G^2 Hermite data consists of end points, tangent vectors and curvatures at those points. In 2006, Yoshida and Saito [17] solved G^1 Hermite interpolation problem which consists of endpoints and tangent vectors at those points. In 2007, Miura et al. extended Yoshida and Saito's work to join LA curve segments with G^2 continuity by changing tangent directions at their joints [13]. However the proposed technique restraints users from specifying tangent directions at the joints. Hence the proposed method cannot solve G^2 Hermite interpolation problem. Up-to-date, no technique exists to design LA curves with G^2 continuity.

There are a number of methods have been proposed to design robot trajectories with clothoid curves [6, 7, 9, 15]. A notable work in this field of study is by Lan et al. [6] who extended Makino's technique [9]. Lan et al. proposed a method to solve the G^2 interpolation problem using clothoid curves. Since the degree of freedom (DOF) of a clothoid is insufficient, they used triple clothoids to obtain the necessary DOFs. As stated previously, clothoid curves are a subset for LA curves when α equals to -1. The DOF of clothoid and LA curve is the same once α is fixed. Hence we extend Lan et al.'s method for LA curve to solve G^2 Hermite interpolation problem using the LA spline which consists of triple LA curve segments connected with G^2 continuity.

The rest of the paper is organized as follows. Section 2 reviews the fundamentals of LA curve and compares two methods to generate a LA curve segment proposed by Yoshida & Saito [17] and Makino [9]. This section also describes a novel method to generate an S-shaped curve with an LA curve segment. Section 3 discusses on the main contribution of this paper; the LA spline formulation to solve G^2 Hermite interpolation problem. Section 4 concludes the paper with a short discussion on future work.

2   GENERATION OF S- SHAPED CURVES USING THE LA CURVES

S-shaped curves are used in various designs and they are very important for aesthetic design [16]. The methods to generate log-aesthetic curves [1, 17] investigated so far do not deal with the input of S-shaped curves since the S-shaped curves can be generated only in the case of α is negative. However the S-shape is inevitable for robots trajectory design. Makino et al. [6, 7, 15] used only clothoid curves (whose α equals to -1 for LA formulation) and their methods can be employed to generate both S-shaped and C-shaped curves. In this section we compare Yoshida & Saito's method [17] to Makino's [9] method and further extend their work to generate S-shaped curves using LA formulation.

2.1   The fundamentals of LA Curves

Referring to Lan et al.'s method [6], the G^2 Hermite interpolation problem for LA spline is formalized based on their notations.

For a given LA curve P, let s and h be its arc length and total length, respectively. $S = s/h (0 \leq S \leq 1)$ represents a dimensionless arc length. The curve is generally expressed by the following equation:

$$P = P_0 = \int_0^s u\, ds = P_0 + h \int_0^S u\, dS,\ 0 \leq s \leq h, 0 \leq S = \frac{s}{h} \leq 1$$

Where P_0 is the start point of the curve and u is its unit tangent vector. Therefore if u is defined as a function of S, the shape of the curve is determined.

In general, a curvature radius function cannot represent a straight line, hence this paper represents   LA curve in the form of curvature function. Frenet-Serret formulas are used for curve shape calculations.

When $\alpha \neq 0$, thesigned curvature of the LA curve, $\kappa(S)$, is defined as follows:

$$\kappa(S) = \begin{cases} (c_0 S + c_1)^{-\frac{1}{\alpha}} & \text{if } c_0 S + c_1 \geq 0 \\ -(-c_0 S - c_1)^{-\frac{1}{\alpha}} & \text{otherwise} \end{cases} \tag{2.1}$$

If the curve is turning left in accord with the direction of travel, the curvature is defined to be positive and negative otherwise. A right-turning curve can also be obtained as a mirror image of a left-turning curve. When $\alpha = 0$, the curvature is given by $\kappa(S) = c_0 e^{c_1 S}$ where its sign is specified by c_0.

Let $\alpha \neq \{0,1\}$ and $c_0 \neq 0$, then the directional angle of the curve, denoted as $\phi(S)$ can be written as follows:

$$\phi(S) = \begin{cases} \dfrac{\alpha}{(\alpha - 1)c_0}(c_0 S + c_1)^{\frac{\alpha-1}{\alpha}} + c_2 & \text{if } c_0 S + c_1 \geq 0 \\[2mm] \dfrac{\alpha}{(\alpha - 1)c_0}(-c_0 S - c_1)^{\frac{\alpha-1}{\alpha}} + c_2 & \text{otherwise} \end{cases} \tag{2.2}$$

where c_2 is an integration constant. Note that in case of $c_0 S + c_1 < 0$, the sign of the first term is without a minus. Hence, it can be rewritten as follows:

$$\phi(S) = \frac{\alpha}{(\alpha - 1)c_0}|c_0 S + c_1|^{\frac{\alpha-1}{\alpha}} + c_2$$

When $c_0 = 0$, the curve is a straight line or an circular arc and its directional angle is defined by

$$\phi(S) = \begin{cases} (c_1)^{-\frac{1}{\alpha}} S + c_2 & \text{if } c_1 \geq 0 \\[2mm] -(-c_1)^{-\frac{1}{\alpha}} S + c_2 & \text{otherwise} \end{cases} \tag{2.3}$$

If $\alpha = 0$, $\phi(S)$ is given by

$$\phi(S) = \frac{c_1}{c_0} e^{c_1 S} + c_2$$

and if $\alpha = 1$, it is given by

$$\phi(S) = \frac{1}{c_0}\log |c_0 S + c_1| + c_2$$

If the curve is a straight line or circular arc, the above equations should be appropriately adjusted.

2.2   Comparison between Yoshida & Saito's Method and Makino's Method

The directional angle of LA curve segment in the standard form II proposed by Yoshida and Saito [17] is given by

$$\phi(s) = \begin{cases} \dfrac{1 - e^{\Lambda s}}{\Lambda} & \text{if } \alpha = 0 \\[3mm] \dfrac{\log(\Lambda s + 1)}{\Lambda} & \text{if } \alpha = 1 \\[3mm] \dfrac{(\Lambda \alpha s + 1)^{\frac{\alpha-1}{\alpha}} - 1}{\Lambda(\alpha - 1)} & \text{otherwise} \end{cases}$$

In this form, the tangent direction at the start point of the curve is assumed to be directed in the positive direction along the x coordinate axis and the curvature radius is assumed to be 1. The curvature radius is increases monotonically when $\Lambda \neq 0$ and when $\Lambda = 0$ in which the curve becomes a circular arc. The shape of the curve is determined by inputting the shape parameter (α) and three points which forms a triangle. The triangle consists of endpoints and an extra point in between of the endpoints which specifies the tangent directions of the endpoints which is similar to control points of a quadratic Bezier curve. A bisection method is used to search for a suitable Λ to match the control points.

Makino [9] used a different approach where the arc length is made to be dimensionless and the start point is translated to be the origin and the end point is rotated to be a point on the x axis whose coordinate is positive. From the directional angles at the start and end points, parameters c_1 and c_2 in Eqn. (2.2) are expressed as linear functions of c_0. The shape of the curve is determined by searching a suitable c_0 which makes the y coordinate of the endpoint to be 0.

The arc length can be made dimensionless by simply excluding the dimension of the curve out of search parameter. It is then fitted with the given control points as proposed by Yoshida and Saito. In essence, both of the discussed methods transforms G^1 Hermite interpolation problem into a one parameter search problem . In Yoshida & Saito's method, Λ is always lower-limited by default and, when $\alpha \neq 1$, Λ is upper-limited. In practice, Yoshida & Saito's method is expected to be advantageous

than the Makino's method. Therefore, we propose a new method to generate a *S*-shape curve based on Yoshida & Saito's method.

It is necessary to connect a number of segments with C^2 continuity to increase the DOF of a LA spline to solve G^2 Hermite interpolation problem. This is due to the fact that the Standard form II proposed by Yoshida and Saito [17] is expressed with a fixed radius curvature at the start point of the segment which makes it impossible to join the subsequent segments with G^2 continuity. Hence, a general formula of LA curve is used to solve the G^2 Hermite interpolation problem and further extend from C^2 continuity to C^n continuity with the LA spline. It is also difficult to estimate the directional angle at the end point of the subsequent segments using Yoshida and Saito's method. Therefore Section 3 is dedicated to formulate a new method solving G^2 Hermite interpolation problem applicable to entire LA family based on the methods proposed by Lan et al. [6] and Makino [7].

2.3   Condition on the LCG gradient to have an inflection point

At an inflection point $(s) = 0$. It is necessary to change the sign of the curvature at a point on the curve to make an *S*-shaped curve, i.e. to have an inflection point where the curvature changes its sign. The curvature of a LA curve in Standard Form II is given by

$$\kappa(s) = \begin{cases} e^{-\Lambda s} & \text{if } \alpha = 0 \\ (\Lambda \alpha s + 1)^{-\frac{1}{\alpha}} & \text{otherwise} \end{cases}$$

The LA curve has no inflection point when $\alpha = 0$ (Nielsen's spiral). If $\alpha > 0$, $\Lambda \alpha s + 1 = \pm\infty$ should be satisfied and inflection point does not occur if the arc length is limited to be finite. Therefore a curve with $\alpha < 0$ may have an inflection point.

2.4   Input of an *S*- shaped Curve

The arc length s of a curve with $\alpha < 0$ is given as a function of the directional angle ϕ at the end point as follows:

$$s = \frac{\{1 + (\alpha - 1)\Lambda\phi\}^{\frac{\alpha}{\alpha-1}} - 1}{\Lambda\alpha} \tag{2.4}$$

It is necessary for the total arc length s to become larger than the arc length to the inflection point s_0 to form a S-shaped curve where

$$s = -\frac{1}{\Lambda\alpha}$$

Notice that $s_0 > 0$ because $\alpha < 0$. If the directional angle is defined to be negative when it decreases over 0 degree, the directional angle becomes maximum at the arc length s_0 and is given by

$$\phi_{max} = \frac{1}{(1-\alpha)\Lambda} \tag{2.5}$$

If the directional angle is specified to be less than the value stated above, it is not possible to generate a curve without a loop which indicates that the directional angle changes by more than 360 º .s is expressed by means of s_0 from Eqn. (2.4) as follows:

$$s = s_0 + \frac{\{1 + (\alpha - 1)\Lambda\phi\}^{\frac{\alpha}{\alpha-1}}}{\Lambda\alpha} \tag{2.6}$$

At the inflection point C^n continuity ($n = 0,1,2\cdots$) of the curve is guaranteed, hence the tangent vector, curvature, derivative of curvature and etc. are continuous. If we assume that the curve is *S*-shaped, the second term of Eqn. (2.6) increases according to the increase of $\phi \to \phi_{max}$. Beyond ϕ_{max} the directional angle (ϕ_D in Fig. 1.) decreases. ϕ_D indicates the directional angle of P_e calculated anticlockwise from x axis and, ϕ_D is the angle between the line through the origin and the P_e and the x axis. Hence we change the sign of the second term and define s_1 by

$$s_1 = -\frac{\{1 + (\alpha - 1)\Lambda\phi\}^{\frac{\alpha}{\alpha-1}}}{\Lambda\alpha} \tag{2.7}$$

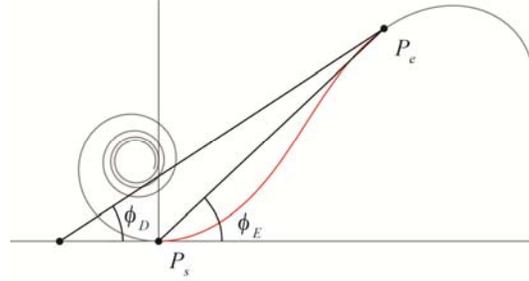Note that since $\alpha < 0$, hence, $s_0 > 0$. The total arc length s is given by $s_0 + s_1$.
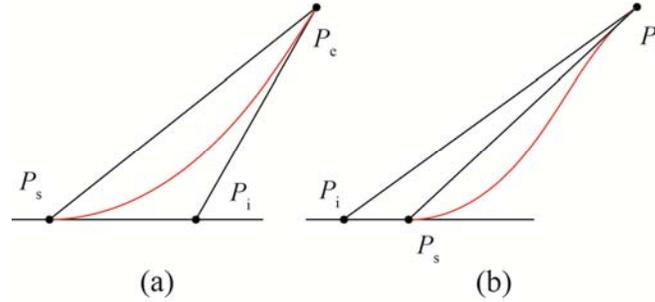
Fig. 1: Input of a S-shaped curve.

Fig. 2: Decision criterion of an S-shape curve.

2.5   An Algorithm to Generate an *S*- shaped LA Curve

We use four control points to generate an *S*-shaped LA curve because if we use only three control points, the two tangent vectors at the start and end points intersect at the second control point unless they are on a line. It is impossible to make the tangent vectors parallel and furthermore, the angle between them negative (clockwise). The four control points are used to specify two end points of the curve and tangent vectors at these points.

An *S*-shaped curve can be generated with the following steps:

1. Move the start point to the origin and the directional angle there to be 0 by translating and rotating the four initial control points,2. Calculate the directional angle at the end point ϕ_D and the angle between the line through the origin and the end point and the x axis ϕ_E as depicted in Fig. 1.,

3. Identify whether the curve is S-shaped from ϕ_D and ϕ_E. A user generates a triangle with the endpoints and the intersection point which dictates tangent vectors endpoints. If the curve exists inside the triangle (Fig. 2(a).), then the curve is identified as an *S*-shaped curve. If the triangle cannot be generated or the curve does not exist inside, then the curve is identified as not an *S*-shaped curve (Fig. 2(a).). If the result is an *S*-shaped curve, then perform the following steps.

4. The minimum value of Λ is 0 and the condition for Λ to satisfy on the maximum directional angle is

$$1 + (\alpha - 1)\Lambda\phi_{max} \geq 0$$

Since $\phi_{max} > 0$, the following inequality is obtained.

$$\Lambda \leq \frac{1}{(1 - \alpha)\phi_{max}}$$

However based on Eqn. (2.5) the above equation is always satisfied, hence no upper-limit exists.

5. Calculate the arc length: $s = s_0 + s_1$ using ϕ_D. (Make sure that $\phi_D < \phi_{max}$.)

6. Calculate the end point of the curve using s and compare the angle corresponding to ϕ_E with itself.

7. If the calculated angle in the previous step is less than ϕ_E, then decrease Λ, otherwise increase it.

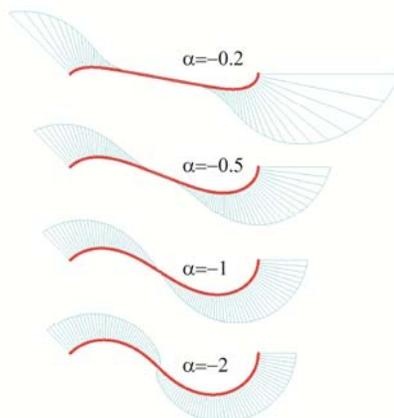8. Repeat steps 5 to 7 until conversion is successful.

Fig. 3: *S*-shaped LA curves with different α values.

In the above algorithm, parameter Λ does not have an upper-limit although it has 0 as the lower-limit and there is not much difference to the Makino's method. However Eqn. (2.7) gives the relationship between the arc length and directional angle. Thus we can avoid a loop whose directional angle grows more than 360 degree.

Fig. 3. shows several examples of *S*-shaped LA curves with different α values. This figure illustrates that the shape of the curve changes very much depending on α when it is S-shaped. All numerical examples illustrated in this paper are performed on a computer built with Core i-7, 3.4 GHz and main memory 8 GB and the average processing time for parameter searching for the *S*-shaped curves in Fig. 3. is about 15 to 20 msec.

3 LOG- AESTHETIC SPLINE WITH THREE SEGMENTS

In this section, we propose to simultaneously specify endpoints, tangent vectors and curvature there using the log-aesthetic spline with three segments which is a similar approach employed by Lan et al. [6] to solve the G^2 Hermite interpolation problem using triple clothoids. Miura et al. [13] used the LCG gradient α, as an additional parameter to make the curvature at the end point to 0. However there is a report which claims α is related to impressions of the curve [4]. Hence, α is fixed as a constant to produce G^1 Hermite interpolation using a single LA curve segment and a C^3 continuous compound-rhythm LA curve is connected with two LA segments. In this paper we regard α as a parameter which can be controlled by designers and do not use it to determine the shape of the curve. Note that the DOF of the LA spline with three segments is similar to triple clothoids.

3.1 Definitions of the LA Spline with Three Segments

Harada et al. [4] reported that α is closely related to impressions of the LA curve. Hence it is a common practice to fix the value of α to design aesthetic shapes using LA curves. We use triple LA curves as a LA spline for the G^2 Hermite interpolation problem. In this paper, a triple LA curve consists of three LA curve segments with different α values which are joined with G^2 continuity. For algebraic simplification we assume that the curve is planar, the curvature of the curve is positive or zero and $\alpha \neq 0, 1$. Let the curvature of LA curve is stated as follows:

$$\kappa(S) = \begin{cases} (c_{10}S + c_{11})^{-\frac{1}{\alpha_1}} & 0 \leq S \leq S_1 \\ (c_{20}S + c_{21})^{-\frac{1}{\alpha_2}} & S_1 < S \leq S_2 \\ (c_{30}S + c_{31})^{-\frac{1}{\alpha_3}} & S_2 < S \leq 1 \end{cases}$$

where S_1 is the normalized arc length defined from 0 to 1 and c_{ij} are constants where i=0,1,2 and j=0,1. S_1 and S_2 can be substituted with any values. However, we use S_1=0.25 and S_2=0.75 as adopted by Lan et al. [6]. When $\{c_{10}, c_{20}, c_{30}\} \neq 0$, the directional angle $\phi(S)$ can be written as follows:

$$\phi(S) = \begin{cases} \dfrac{\alpha_1}{(\alpha_1 - 1)c_{10}}(c_{10}S + c_{11})^{\frac{\alpha_1 - 1}{\alpha_1}} + c_{12} & 0 \leq S \leq S_1 \\ \dfrac{\alpha_2}{(\alpha_2 - 1)c_{20}}(c_{20}S + c_{21})^{\frac{\alpha_2 - 1}{\alpha_2}} + c_{22} & S_1 < S \leq S_2 \\ \dfrac{\alpha_3}{(\alpha_3 - 1)c_{30}}(c_{30}S + c_{31})^{\frac{\alpha_3 - 1}{\alpha_3}} + c_{32} & S_2 < S \leq 1 \end{cases}$$

In case of $\kappa(S) < 0$, the curvature and directional angle can be defined similar to Eqn. (2.1) and Eqn. (2.2), respectively.

3.2   Conditions on Segments

The conditions for satisfying the imposed constraints at endpoints and to preserve G^2 continuity at the joints of the triple LA curves are given by:

$$\kappa_s h = (c_{11})^{-\frac{1}{\alpha_1}} \tag{3.1}$$

$$\kappa_e h = (c_{30} + c_{31})^{-\frac{1}{\alpha_3}} \tag{3.2}$$

$$\phi_s = \frac{\alpha}{(\alpha - 1)c_{10}}(c_{11})^{\frac{\alpha_1 - 1}{\alpha_1}} + c_{12} \tag{3.3}$$

$$\phi_e = \frac{\alpha}{(\alpha - 1)c_{30}}(c_{30} + c_{31})^{\frac{\alpha_3 - 1}{\alpha_3}} + c_{32} \tag{3.4}$$

Note that although for an arbitrary α_1 and α_3, Eqns. (3.1) and (3.2) can be rewritten as linear functions of $c_{ij}(i = 1,2,3, j = 0,1,2)$, however Eqns. (3.3) and (3.4) cannot be linear functions when $\alpha_1, \alpha_3 \neq -1$.

The conditions to preserve curvature continuity and the directional angle at the two joints are given by

$$(c_{10}S_1 + c_{11})^{-\frac{1}{\alpha_1}} = (c_{20}S_1 + c_{21})^{-\frac{1}{\alpha_2}} \tag{3.5}$$

$$(c_{20}S_2 + c_{21})^{-\frac{1}{\alpha_2}} = (c_{30}S_2 + c_{31})^{-\frac{1}{\alpha_3}} \tag{3.6}$$

$$\frac{\alpha_1}{(\alpha_1 - 1)c_{10}}(c_{10}S_1 + c_{11})^{\frac{\alpha_1 - 1}{\alpha_1}} + c_{12} = \frac{\alpha_2}{(\alpha_2 - 1)c_{20}}(c_{20}S_1 + c_{21})^{\frac{\alpha_2 - 1}{\alpha_2}} + c_{22} \tag{3.7}$$

$$\frac{\alpha_2}{(\alpha_2 - 1)c_{20}}(c_{20}S_2 + c_{11})^{\frac{\alpha_2 - 1}{\alpha_2}} + c_{22} = \frac{\alpha_3}{(\alpha_3 - 1)c_{30}}(c_{30}S_2 + c_{31})^{\frac{\alpha_3 - 1}{\alpha_3}} + c_{32} \tag{3.8}$$

Eqns. (3.7) and (3.8) are essentially non-linear. Eqns. (3.5) and (3.6) are simplified as follows:

$$c_{20}S_1 + c_{21} = (c_{10}S_1 + c_{11})^{\frac{\alpha_2}{\alpha_1}} \tag{3.9}$$

$$c_{20}S_2 + c_{21} = (c_{30}S_2 + c_{31})^{\frac{\alpha_2}{\alpha_3}} \tag{3.10}$$

Let the coordinates of the endpoint of the curve be $(r, 0)$, the following two equations should be satisfied.

$$h \int_0^1 \cos\phi(S)\, dS = r \tag{3.11}$$

$$\int_0^1 \sin\phi(S)\, dS = 0 \tag{3.12}$$

The variables are h and c_{ij} with $\{i = 1,2,3, j = 0,1,2\}$ and the number of unknown is 10 in the above formulation. The conditions are from Eqn. (3.1) to (3.4) and from Eqn. (3.7) to (3.12). The number of them adds to 10 as well. Hence the number of unknowns and equation are the same and which makes a determined system.

3.3 Proposed Solution

At first we estimate the total length h and express the left side of Eqn. (3.12) by only c_{30}. Its value is determined by binary search algorithm to satisfy Eqn. (3.12). From Eqn. (3.11), h is calculated by using c_{30}. The process is repeated until the iteration converges to the solution.

We assume that c_{30} is given as a numerical value due to the fact that both c_{10} and c_{30} remain as unknown. If we can treat c_{30} as a numerical value, we obtain c_{10} by solving a nonlinear equation. Then we may update the value of c_{30} to satisfy constraints without c_{10}.

From Eqn. (3.1) to Eqn. (3.4)

$$c_{11} = (\kappa_s h)^{-\alpha_1} \tag{3.13}$$
$$c_{31} = (\kappa_e h)^{-\alpha_3} - c_{30} \tag{3.14}$$
$$c_{12} = \phi_s - \frac{\alpha_1}{(\alpha_1 - 1)c_{10}}(\kappa_s h)^{1-\alpha_1} \tag{3.15}$$
$$c_{32} = \phi_e - \frac{\alpha_3}{(\alpha_3 - 1)c_{30}}(\kappa_e h)^{1-\alpha_3} \tag{3.16}$$

Hence c_{31} and c_{32} are determined by c_{30} and c_{12} using c_{10}.

From Eqns. (3.9) and (3.10)

$$\begin{bmatrix} S_1 & 1 \\ S_2 & 1 \end{bmatrix} \begin{bmatrix} c_{20} \\ c_{21} \end{bmatrix} = \begin{bmatrix} (c_{10}S_1 + c_{11})^{\frac{\alpha_2}{\alpha_1}} \\ (c_{30}S_2 + c_{31})^{\frac{\alpha_2}{\alpha_3}} \end{bmatrix}$$

Therefore

$$c_{20} = \frac{(c_{10}S_1 + c_{11})^{\frac{\alpha_2}{\alpha_1}} - (c_{30}S_2 + c_{31})^{\frac{\alpha_2}{\alpha_3}}}{S_1 - S_2} \tag{3.17}$$

$$c_{21} = \frac{S_1(c_{30}S_2 + c_{31})^{\frac{\alpha_2}{\alpha_3}} - S_2(c_{10}S_1 + c_{11})^{\frac{\alpha_2}{\alpha_1}}}{S_1 - S_2} \tag{3.18}$$

By using Eqns. (3.7) and (3.8) we remove c_{22} as follows:

$$\frac{\alpha_1}{(\alpha_1 - 1)c_{10}}(c_{10}S_1 + c_{11})^{\frac{\alpha_1-1}{\alpha_1}} + c_{12} + \frac{\alpha_2}{(\alpha_2 - 1)c_{20}}\{(c_{20}S_2 + c_{11})^{\frac{\alpha_2-1}{\alpha_2}} - (c_{20}S_1 + c_{21})^{\frac{\alpha_2-1}{\alpha_2}}\} - \frac{\alpha_3}{(\alpha_3 - 1)c_{30}}(c_{30}S_2 + c_{31})^{\frac{\alpha_3-1}{\alpha_3}} - c_{32} = 0$$

We define the left side of the above equation as $f(c_{10})$. c_{12}, c_{20} and c_{21} are functions of c_{10} and from Eqns. (3.13), (3.15) and (3.16) we obtain the following equations when $\alpha_2/\alpha_1 \neq -1$:

$$\frac{\partial c_{12}}{\partial c_{10}} = \frac{\alpha_1}{(\alpha_1 - 1)c_{10}^2} c_{11}^{\frac{\alpha_1-1}{\alpha_1}}$$

$$\frac{\partial c_{20}}{\partial c_{10}} = \frac{S_1}{S_1 - S_2}\frac{\alpha_2}{\alpha_1}(c_{10}S_1 + c_{11})^{\frac{\alpha_2}{\alpha_1}-1}$$

$$\frac{\partial c_{21}}{\partial c_{10}} = -\frac{S_1 S_2}{S_1 - S_2}\frac{\alpha_2}{\alpha_1}(c_{10}S_1 + c_{11})^{\frac{\alpha_2}{\alpha_1}-1}$$

We can also obtain similar formulas when $\alpha_2/\alpha_1 = -1$. Hence we can numerically evaluate $\partial f(c_{10})/\partial c_{10}$. Since differentiation is possible, we can adopt numerical methods using derivatives such as the Newton's method to solve a non-linear equation by forming $f(c_{10}) = 0$. Although the method described above assumes that $\alpha \neq \{0,1\}$ it is possible to formulate similar solution for such cases.

3.4   Initial Value Estimation

We need initial values for h, c_{10} and c_{30} in the proposed solution. To obtain the initial values for c_{10} and c_{30}, we estimate curvatures at the joints at S_1 and S_2 and calculate them from these curvatures.

We may use a Bézier curve of degree 5 for the estimation of the initial shape of the LA spline. We can use the total length of the Bézier curve as h. To note, the Bézier curve is not uniquely determined by endpoints, tangent directions and curvatures there and these conditions do not necessarily yield a suitable curve for the initial value estimation for c_{10} and c_{30}.

Hence we use an objective function which is modified to be independent from the total length h as proposed by Miura at al. [13]:

$$J_{LAC} = \frac{\int_0^{S_1 h} \sqrt{1 + \alpha_1^2 \rho^{2\alpha_1 - 2} \rho_s^2}\, ds + \int_{S_1 h}^{S_2 h} \sqrt{1 + \alpha_2^2 \rho^{2\alpha_2 - 2} \rho_s^2}\, ds + \int_{S_2 h}^{h} \sqrt{1 + \alpha_3^2 \rho^{2\alpha_3 - 2} \rho_s^2}\, ds}{h} \tag{3.19}$$

The above function is minimized to generate an appropriate initial Bézier curve. Fig. 4(a). shows a Bézier curve of degree 5 and its initial control points in green and those after optimization in blue for $\alpha_i = -0.5$, $i = 1,2,3$.
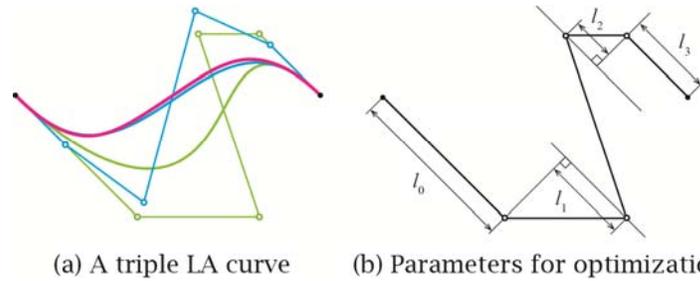

(a) A triple LA curve   (b) Parameters for optimization

Fig. 4: Optimization of the approximation curve for initial values.

Upon using the Bézier curve after optimization, c_{10} and c_{30} are calculated and a LA spline curve with three segments shown in red is determined. Strictly speaking the LA spline curve does not minimize the objective function in Eqn. (3.19), but notice that the shapes of the Bézier curve and the LA spline are almost in the same shape.

In this example, c_{10} and c_{30} calculated from the input Bézier curve are not appropriate, hence the numerical calculation diverges because the total length h becomes negative. If we use the Bezier curve after optimization, we may obtain these values without calculation failure and generate a LA spline curve successfully.

Since an optimization process is necessary only for the initial value estimation, we propose a simpler method. As shown in Fig. 4(b). let the lengths between the first and the second control points and the fifth and sixth control points be l_0 and l_3, respectively. Furthermore let parameters to determine the positions of the 3rd and 4th be l_1 and l_2, respectively. We change these parameters independently in the range of $0.05 \leq \frac{l_i}{h} \leq 0.5$ for , $i = 0,1,\cdots,3$ by 0.05 where h is the total arc length of the input Bézier curve. We obtain parameter values which minimizes the objective function in Eqn.(3.19).
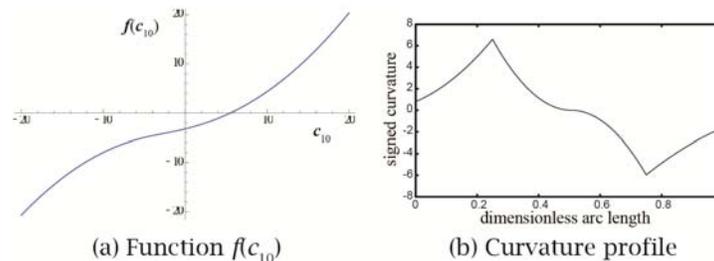

(a) Function $f(c_{10})$ (b) Curvature profile

Fig. 5: (a)Non-linearity of function $f(c_{10})$, (b) the curvature profile of the LA spline curve with three segments shown in Fig. 4(a).

Figure 5. shows function $f(c_{10})$ defined in the previous subsection calculated by using the initial values obtained from the optimized Bézier curve of degree 5. We notice from the figure that the function is non-linear, but there is only one solution which satisfies $f(c_{10}) = 0$ in the range of $-20 \leq c_{10} \leq 20$. Figure 6. shows a curvature profile of the LA spline curve. Its curvature is continuous for the whole curve, but the monotonicity is not preserved because the specified curvatures at the end points are relatively small. The processing time is about 30 msec for the optimization process and about 20 msec for the parameter search, adding to 50 msec.
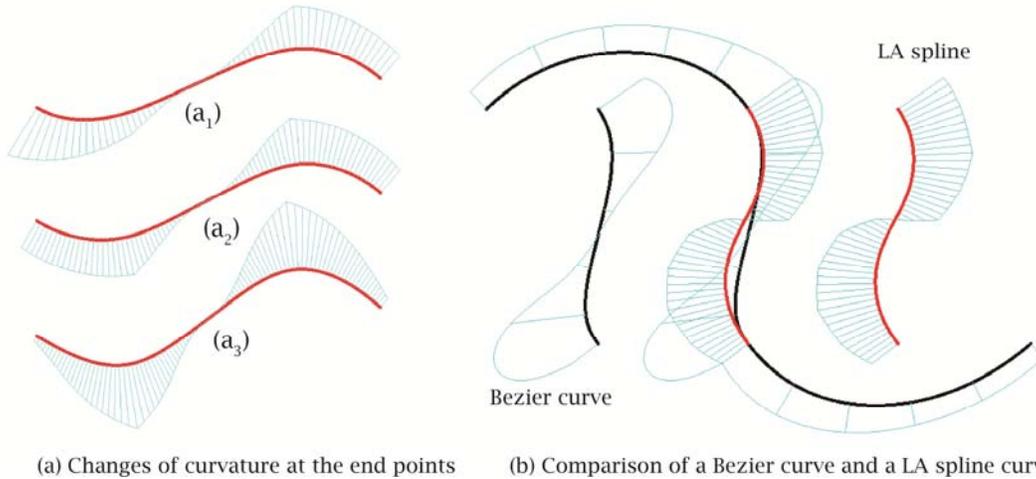
(a) Changes of curvature at the end points   (b) Comparison of a Bezier curve and a LA spline curve

Fig. 7: (a) LA splines with different curvatures at the end points ($\alpha = -0.5$), (b) a generation of G^2 continuous Bézier curve of degree five satisfying traditional G^2 Hermite data by a built-in command with and a LA spline in red color with the same G^2 Hermite data .

Figure 7(a). shows examples of LA spline for different curvatures at their end points. Even though the curvature of the curve in Fig. 7(a_1). appears to be monotonous, generally it is not guaranteed to be monotonous as depicted in Fig. 7(a_2). and 7(a_3). In Fig. 7(b). the central curve consists of three segments whose middle segment is generated using Bézier curve of degree 5 (black) and a LA spline (red) in using the proposed method. The Bézier curve is generated and deformed by built-in commands of a commercial CAD system to satisfy G^2 Hermite data posed at its endpoints. The LA spline is generated with similar G^2 Hermite data to achieve G^2 continuity at the joints. These curves are also shown separately for visual clarity. The porcupine plot of these curves is drawn in blue. It is visually clear that the curvature of the Bézier curve varies a lot to satisfy G^2 continuity at its endpoints whereas LA spline joins gradually.
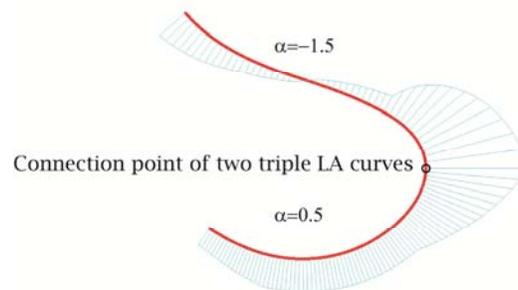

Fig. 8: A G^2 connection example of two LA spline curves.

We show an example to connect two LA spline curves with different α values with G^2 continuity in Fig. 8. Our method can connect LA spline with G^2 continuity if the same curvatures are specified at their connection points. The average processing time to generate this spline is about 35 msec.
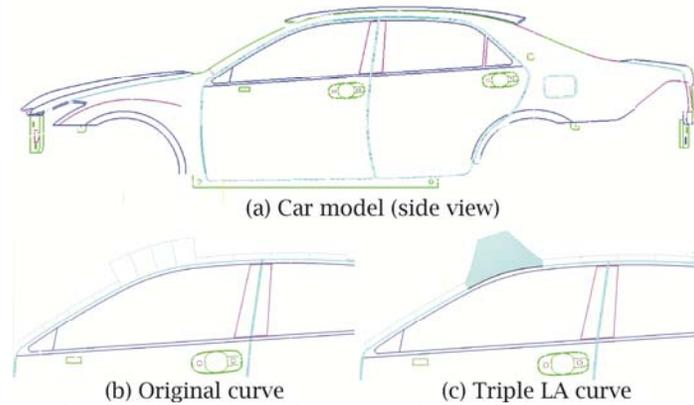
Fig. 9: Circular arc replacement by a LA spline to achieve G^2 continuity.

Figure 9. shows a replacement of an arc in a practical CAD data to achieve G^2 continuity. The curvature of three curves at the upper position of a front door in Fig. 9(a). is not continuous as shown in Fig. 9(b). The circular arc is replaced with a LA spline and the result indicates the curvature is continuous as shown in Fig. 9(c).
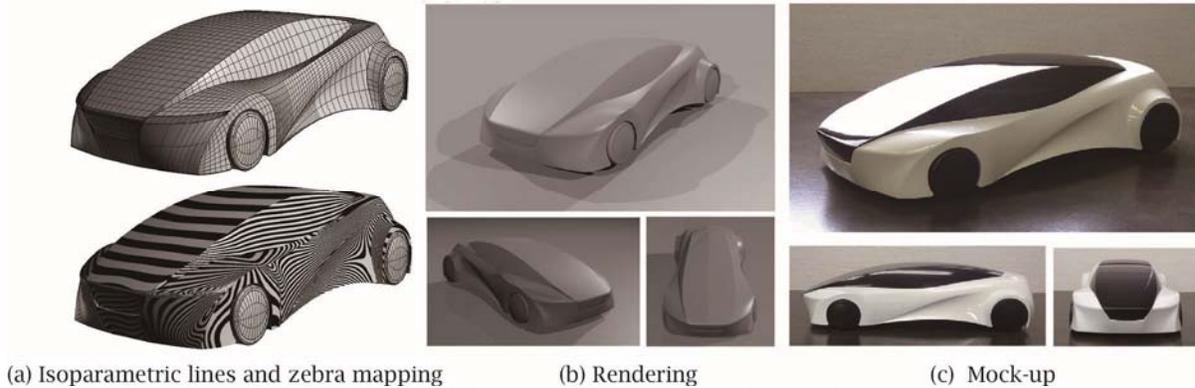
Fig. 10: A car model designed by using LA spline and its mock-up.

Figure 10. shows a practical design example of a car designed by using LA splines. Figure 10(a). shows iso-parametric lines of free-form surface generated using LA splines and its corresponding zebra maps. Figure 10(b). depicts the geometric model with special lighting condition and 10(c). are photos of its mock-up manufactured based on geometric model. To note, the roof of the car is designed by a LA spline curve with three segments and its zebra maps indicates the surface is of high quality.

Although to find out drawable regions of our method is one of future researches, our experiences indicate the regions are very wide and we can generate LA splines for practical with most of G^2 Hermite data.

4   CONCLUSIONS

The contribution of this paper is twofold: the first part proposed a novel method to generate a *S*-shaped LA curve which deals with G^1 Hermite interpolation problem. The second part proposes a new method to solve G^2 Hermite interpolation problem with LA curves. These methods have been successfully implemented as a plug-in module for a commercial CAD system and are found to be essential for practical design. It is hoped that complex aesthetic shapes which assumed hard to design can be designed easily using the proposed methods with minimal effort.

REFERENCES

[1]   Agari, S.; Miura, K.T.; Fujisawa, M.: Nisikawa, T.; Hada, T.: Input of the compound-rhythm log-aesthetic curve and its applications for styling design, Journal of Japan Society of Mechanical Engineers, 75(756), 2009, 2159-2164, (Japanese).
[2]   Gobithaasan, R.U.; Miura, K.T.: Aesthetic spiral for design, Sains Malaysiana, 40(11), 2011, 1301-1305.
[3]   Gobithaasan, R.U.; Md. Ali; J.; Miura, K.T.: The elucidation of planar aesthetic curves, 17th International Conference in Central Europe on Computer graphics, Visualization and Computer Vision, WSCG'2009, 138-188.
[4]   Harada, T.; Yoshimoto, F.; Moriyama, M.: An aesthetic curve in the field of industrial design, Procs. IEEE Symposium on Visual Language 1999, 38-47.
[5]   Jamaludin, M.A.; Tookey, R.M.; Ball, J.V.; Ball, A.A.: The generalized cornu spiral and its application to span generation, Journal of Computational and Applied Mathematics, 102(1), 1999, 37-47.
[6]   Lan, F.; Tamai, H.; Makino, H.: Interpolation of arbitrary point sequence by triple clothoid curves, Journal of the Japan Society for Precision Engineering, 76(10), 2010, 1194-1199, (Japanese).
[7]   Lan, F.; Tamai, H.; Miura, K.T.; Makino, H.: Path generation using linear curvature and torsion segments, Journal of the Japan Society for Precision Engineering, 78(7), 2012, 605-610, (Japanese).
[8]   Levien, R.: From Spiral to Spline: Optimal Techniques in Interactive Curve Design, Ph.D. Thesis, The University of California, Berkeley, 2009.
[9]   Makino, H.: Clothoidal interpolation of freely given point series using tangent method, Journal of the Japan Society for Precision Engineering, 60(1), 1994, 80-85, (Japanese).
[10]   Meek, D.S.; Saito, T.; Walton, D.J.; Yoshida, Y.: Planar two-point G1 Hermite interpolating log-aesthetic spirals, Journal of Computational and Applied Mathematics, 236(17), 2012, 4485-4493.
[11]   Miura, K.T.; Fujisawa, M.; Nishikawa, S.; Hada, T.: Extension of the aesthetic curves into 3-dimensional space and their approximation by B-spline curves, Proc. Graphics and CAD/Visual Computing Joint Symposium 2006 , 83-88, (Japanese).
[12]   Miura, K.T.: A general equation of aesthetic curves and its self-affinity, Computer-Aided Design & Applications , 3(1-4), 2006, 457-464.
[13]   Miura, K.T.; Yagi, M.; Kawata, Y.; Fujisawa, M.: Input of aesthetic curve segments with inflection end points and generation of aesthetic curves with G2 continuity, Proc. Graphics and CAD/Visual Computing Joint Symposium 2007 , 297-302, (Japanese).
[14]   Miura, K.T.; Shirahata, R.; Agari, S.; Usuki, S.; Gobithaasan, R.U.: Variational formulation of the log-aesthetic surface and development of discrete surface filters, Computer-Aided Design and Applications, 9, 6, (2012) 901-914.
[15]   Qiu, S.Y.; Makino, H.; Suda, H.; Yokoyama, Y.: Free curve interpolation using clothoidal curve, Journal of the Japan Society for Precision Engineering, 8(6), 1990, 680-687, (Japanese).
[16]   Takanashi, T.: Aesthetic design methodology, David publishing, 2002, (Japanese).
[17]   Yoshida, N.; Saito, T.: Interactive aesthetic curve segments, The Visual Computer (Pacific Graphics), 22(9-11), 2006, 896-905.
[18]   Ziatdinov, R.; Yoshida, N; Kim, T.: Analytic parametric equations of log-aesthetic curves in terms of incomplete gamma functions, Computer Aided Geometric Design, 29(2), 2012, 129-140.